



## Temporal correlation of elevated *PRMT1* gene expression with mushroom body neurogenesis during bumblebee brain development



Cui Guan, Michaela Egertová, Clint J. Perry, Lars Chittka, Alexandra Chittka\*

School of Biological and Chemical Sciences, Queen Mary University of London, Mile End Road, London E1 4NS, UK

### ARTICLE INFO

#### Keywords:

Arginine methylation  
Insects  
Neural development  
Mushroom body  
PRMT

### ABSTRACT

Neural development depends on the controlled proliferation and differentiation of neural precursors. In holometabolous insects, these processes must be coordinated during larval and pupal development. Recently, protein arginine methylation has come into focus as an important mechanism of controlling neural stem cell proliferation and differentiation in mammals. Whether a similar mechanism is at work in insects is unknown. We investigated this possibility by determining the expression pattern of three protein arginine methyltransferase mRNAs (*PRMT1*, 4 and 5) in the developing brain of bumblebees by *in situ* hybridisation. We detected expression in neural precursors and neurons in functionally important brain areas throughout development. We found markedly higher expression of *PRMT1*, but not *PRMT4* and *PRMT5*, in regions of mushroom bodies containing dividing cells during pupal stages at the time of active neurogenesis within this brain area. At later stages of development, *PRMT1* expression levels were found to be uniform and did not correlate with actively dividing cells. Our study suggests a role for PRMT1 in regulating neural precursor divisions in the mushroom bodies of bumblebees during the period of neurogenesis.

### 1. Introduction

The development of insects includes embryonic and postembryonic stages. The embryonic stage corresponds to the egg, whereas post-embryonic stages of holometabolous insects comprise those of the larva, the pupa and the adult. During the development of holometabolous insects, the brain changes drastically not only in size but also in structure, especially during the larval and pupal stages (Farris et al., 1999). Prominent structures of the insect brain are the optic lobes (visual system), antennal lobes (olfactory system) (Groh and Rössler, 2008), the central complex (which plays an essential role in sky-compass orientation (Held et al., 2016) and aversive colour learning in honeybees (Plath et al., 2017), and in other insects regulates a wide repertoire of behaviours including locomotion, stridulation, spatial orientation and spatial memory (Neuser et al., 2008; Pan et al., 2009)), and higher order centres that coordinate sensory integration called the mushroom bodies (MBs) (Bullock and Horridge, 1965; Chittka and Niven, 2009; Hanström, 1928). The mushroom bodies, which have been compared to the mammalian hippocampus, cerebellum and the piriform cortex, are paired brain structures responsible for learning and memory functions in insects (Heisenberg, 1998; Li et al., 2018). In the adult brain, each mushroom body consists of two cap-like structures, called calyces (Rybak and Menzel, 2010), comprised of the dendrites of

a large number of densely packed neurons, termed Kenyon cells (Farris et al., 1999; Kenyon, 1896; Rybak and Menzel, 2010). The cell bodies of most Kenyon cells are enclosed by the calyces, while few are on the sides of or underneath the calyces (Farris et al., 1999; Kenyon, 1896; Rybak and Menzel, 2010).

During development of honeybees, neuroblasts located at the centre of the cups of the calyces (neuroblast clustered regions, termed proliferative regions), divide and produce Kenyon cells (Farris et al., 1999; Kurshan et al., 2003; Malun, 1998). The neuroblasts begin their division from the first larval instar stage (four days from egg laying), continuing until the mid-late pupal stage (approximately five days from pupation, 16 days from egg laying) (Farris et al., 1999).

The first described mechanism for neural precursor divisions in insects involves so called Type I neuroblasts. These neuroblasts divide asymmetrically to proliferate and produce a ganglion mother cell (GMC) which undergoes a single symmetric division to produce two neurons (Farris et al., 1999). An additional type of neuroblast (type II neuroblasts) has been identified in *Drosophila* (Homem and Knoblich, 2012). Type II neuroblasts divide asymmetrically to renew themselves and generate a transit amplifying intermediate neural progenitor that continues to renew itself three to five times to generate more transit amplifying intermediate neural progenitors and a GMC that divides again to generate two neurons (Homem and Knoblich, 2012). The types

\* Corresponding author.

E-mail address: [a.chittka@qmul.ac.uk](mailto:a.chittka@qmul.ac.uk) (A. Chittka).

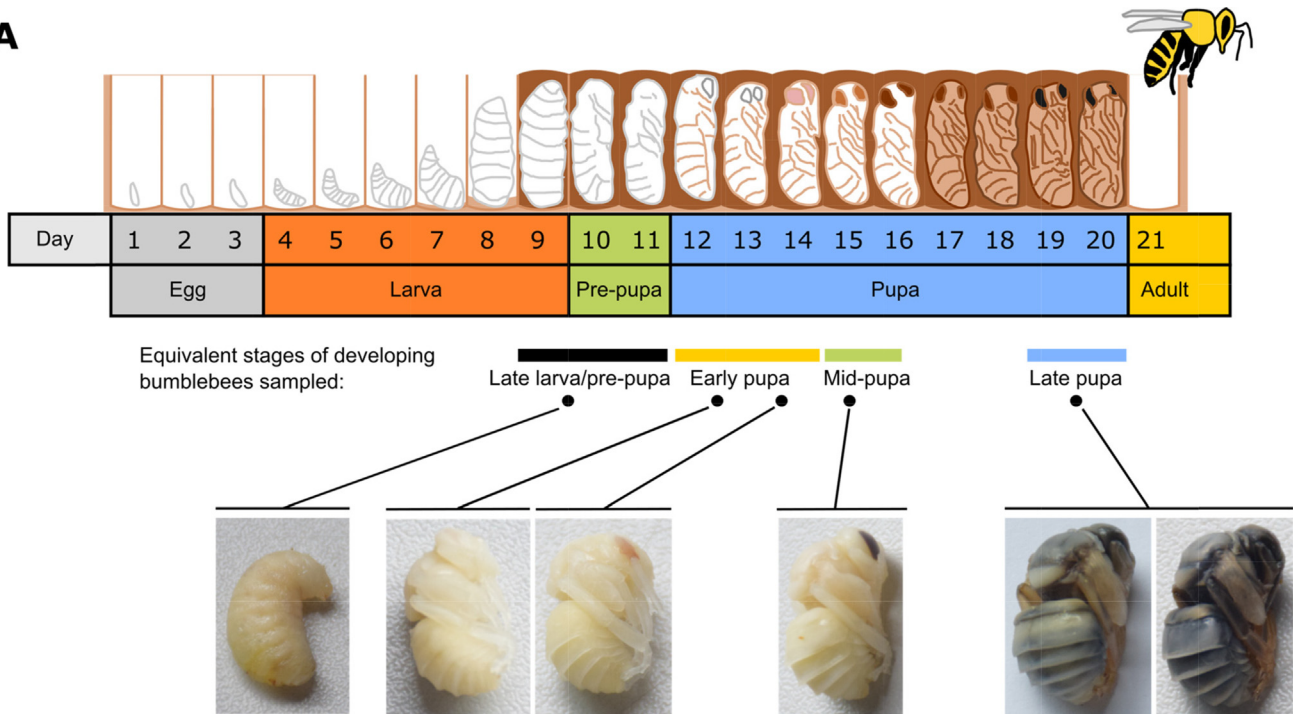
<https://doi.org/10.1016/j.jinsphys.2019.04.011>

Received 23 November 2018; Received in revised form 21 April 2019; Accepted 26 April 2019

Available online 27 April 2019

0022-1910/ © 2019 Elsevier Ltd. All rights reserved.

**A**



**B**

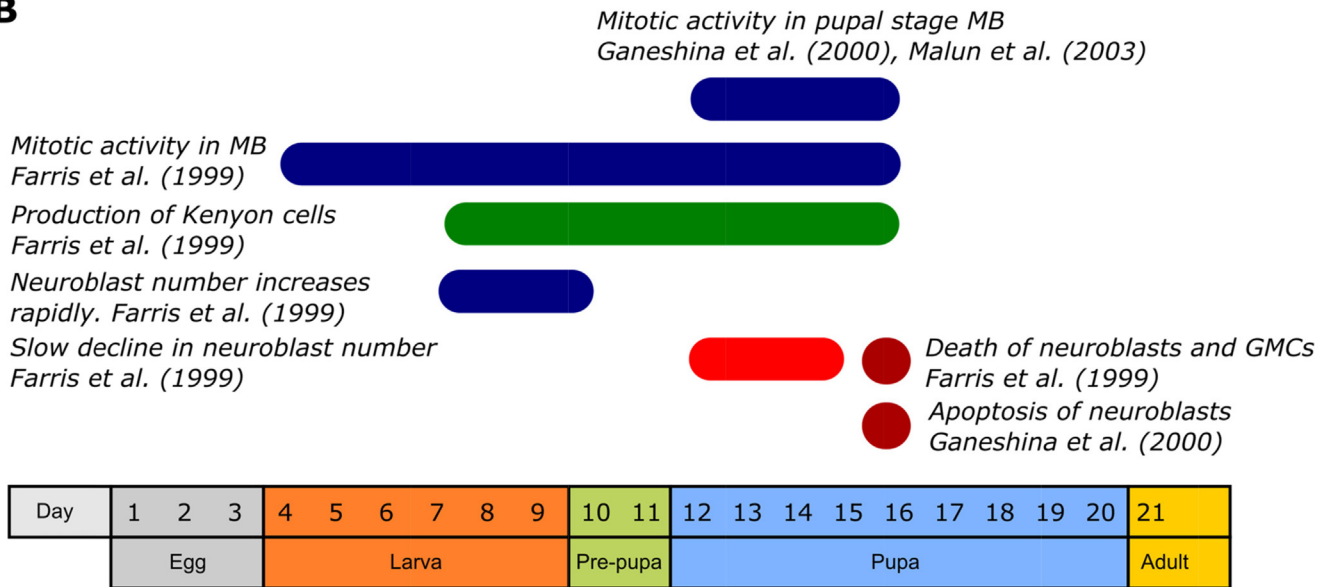


**Fig. 1.** Developmental stages of honeybees and bumblebees and the corresponding changes in the composition of developing mushroom bodies (MBs). A) Schematic diagram of different developmental stages of honeybee and the equivalent stages of bumblebees investigated in this study. Given the highly close genetic and anatomic similarity between honeybees and bumblebees, eye colour and head pigmentation were used in the present study as markers to determine the equivalent bumblebee developmental stages to those stated in honeybee literature. Late larva/Pre-pupa in bumblebees correspond to days 9–11 of honeybee development; early pupa in bumblebees correspond to days 12–14 of honeybee developmental; mid-pupa in bumblebees corresponds to approximately day 15–16 honeybee developmental stage; the late bumblebee pupa corresponds to day 19–20 of honeybee development. B) Schematic diagram of reported cell division, differentiation and apoptosis during the development of mushroom bodies of honeybees. Farris *et al.* showed that there was mitotic activity in the mushroom bodies from day 4 until day 16 of development; newly produced Kenyon cells were visible from day 7 until day 16 of development; the number of mushroom body neuroblasts increases drastically from day 7 until day 9 of development, and slowly declines from day 12 to day 15 of development; cell death of neuroblasts and ganglion mother cells (GMCs) started on day 15 and was evident on day 16 of development (Farris *et al.*, 1999). From day 12 to day 16 of development, Ganeshina *et al.* and Malun *et al.* detected mitotic activity of cells in mushroom bodies (Ganeshina *et al.*, 2000; Malun *et al.*, 2003). Ganeshina *et al.* showed that there were apoptotic cells from day 15 of development onwards and extensive apoptosis was observed on day 16 of development (Ganeshina *et al.*, 2000).

of neuroblasts present in the developing nervous system of the bumblebee are unknown. In honeybees, Farris et al. 1999 found Type I neuroblasts, but no evidence of other division patterns in the mushroom body; in fruit flies, there are no type II neuroblast divisions in the embryonic mushroom body, as judged by a lack of cells expressing a marker of transit amplifying intermediate neural progenitors. It is thus likely that type I neuroblasts are the major neuroblast in the mushroom bodies of bumblebees (Farris et al., 1999; Kunz et al., 2012).

In the developing bee, neural precursor division and neurogenesis cause a dramatic change in the cytoarchitecture of mushroom bodies (Farris et al., 1999). During the larval and pre-pupal stages the neuropils begin to form with the peduncular neuropil first observable during the third larval instar (six days from egg laying) and the calycal neuropils first seen during the pre-pupal stage (10–11 days from egg laying) (Kurshan et al., 2003). Normally at pupal day 5, neurogenesis in the mushroom bodies of bees cease (Farris et al., 1999). However, the growth of the mushroom body neuropil does not cease but continues throughout adult life (Farris et al., 2001). The developmental stages of worker honeybees and bumblebees are shown in Fig. 1A, and a description of previously-reported patterns of cell division, differentiation and apoptosis during the development of mushroom bodies of honeybees is shown in Fig. 1B. These neuroanatomical changes during bee development are well defined, but less is known about their molecular basis.

Post-translational modifications of proteins play an important role in modulating their function, their interactions with various partners as well as their subcellular localisation. Different types of post-translational modifications thus fine-tune cellular responses to various environmental cues during development, allowing for stage-specific responses. Recent work has highlighted the importance of protein arginine methyltransferases (PRMTs) in regulating the development of the nervous system in vertebrates. PRMTs are a family of enzymes that catalyse the transfer of a methyl group from S-adenosylmethionine (SAM) to the guanidine nitrogen atoms of arginine (Blanc and Richard, 2017; Krause et al., 2007) leading to the generation of monomethyl, symmetric or asymmetric dimethyl arginines (MMA, SDMA and ADMA, respectively). ADMA is mediated by type I PRMTs, which include PRMT1, 2, 3, 4, 6 and 8, whereas SMDA is mediated by type II PRMTs, represented by PRMT5 and 9 (Bedford and Clarke, 2009; Wang and Li, 2012). PRMTs control a multitude of essential cellular processes, e.g., cell proliferation and differentiation in all tissues during development, through the modification of protein substrates (Blackwell and Ceman, 2012; Hirota et al., 2017; Kimura et al., 2008; Pawlak et al., 2000; Takahashi et al., 2011; Tee et al., 2010; Wang and Li, 2012; Yadav et al., 2003). Their roles in controlling neural development in vertebrates are beginning to be elucidated (Hein et al., 2015; Huang et al., 2011; Selvi et al., 2015; Simandi et al., 2015). For example, PRMT1 has been implicated in neurite outgrowth in human neuro2a cells during neuronal differentiation (Miyata et al., 2008) and in the switch between epidermal and neural fate in *Xenopus* embryos (Batut et al., 2005). Interestingly, enzymatic activity of PRMT1 is upregulated by the rodent antiproliferative protein TIS21 (Lin et al., 1996), a marker of all neural progenitors that are undergoing neurogenic divisions during mammalian development (Canzoniere et al., 2004; Haubensak et al., 2004; Iacopetti et al., 1999). CARM1/PRMT4 regulates proliferation of PC12 cells, the cell line which is responsive to the proliferation-inducing Epidermal Growth Factor (EGF) and the differentiation-inducing Nerve Growth Factor (NGF) (Greene and Tischler, 1976), by methylating the RNA binding protein HuD and controlling the choice of cell-cycle specific mRNAs bound by HuD in this manner (Fujiwara et al., 2006). PRMT5 maintains neural stem cell proliferation during early stages of development and its activity is downregulated by NGF in PC12 cells (Chittka, 2013; Chittka et al., 2012). Moreover, neural stem cell specific ablation of *PRMT5* in mice revealed its role in maintaining neural stem cell homeostasis during development (Bezzi et al., 2013).

Together, the emerging information underscores the importance of

protein arginine methylation during neural development. However, very little is known about the role that PRMTs may play in insect neural development. To address the potential roles of PRMTs in bumblebee neural development, in the first instance we set out to investigate the mRNA expression of these genes within the developing central nervous system (CNS) at different developmental stages. We focused our study on *PRMT1*, *PRMT4* and *PRMT5* because previous studies showed that they are important in the vertebrate nervous system development and their sequences are conserved across different species, from *Drosophila melanogaster* to mammals (Batut et al., 2005; Bedford and Clarke, 2009; Chittka, 2013; Chittka et al., 2012; Fujiwara et al., 2006; Miyata et al., 2008; Wang and Li, 2012).

## 2. Materials and methods

### 2.1. Collection of bees

An overview of the methods in this study and general protocol is given in Supplementary Fig. S1. Bees from three *Bombus terrestris* colonies (Biobest Belgium N.V., Westerlo, Belgium) were maintained at Queen Mary University of London (Mile End campus). Pollen (approximately 7 g) and 30% sucrose (w/v) were given *ad libitum* to the hive every day during the experiment. The life cycle of a bee consists of four major stages: egg, larva, pupa, and finally the adult. Generally speaking, for a *Bombus terrestris* worker bee, eggs hatch into larvae after 4–6 days (Prŷs-Jones and Corbet, 2003). The larval stage lasts for 10–20 days before it pupates. Then the larva moults and spins a silken cocoon around its body. After about two weeks as a pupa, an adult worker emerges (Prŷs-Jones and Corbet, 2003). Six developmental stages of bees were collected. These were late larvae/pre-pupae (with the larva ceasing any movements and the cocoon being formed), early-pupae (white/pink eye pupae), mid-pupae (brown eye pupae), late pupae (the cocoon contains a black body and head), two-day old workers, and seven to ten-day old workers. Given the highly close genetic and anatomic similarity between honeybees and bumblebees (Riveros and Gronenberg, 2010; Stolle et al., 2011), eye colour and head pigmentation were used in the present study as markers to sample the pupal staged bees based on the honeybee literature (Fig. 1A) (Jay, 1962). Two-day old workers were sampled because this is the earliest age a worker bee can start to forage (Pouvreau, 1989). Furthermore, two-day old worker honeybees without flight experience go through a drastic outgrowth of Kenyon cell dendrites in mushroom bodies (Durst et al., 1994; Fahrbach et al., 1998; Farris et al., 2001). Seven to ten-day old workers were sampled because this range was the average age for a bumblebee to start to forage according to the present experimental observations. All the bees were kept inside the nest without any flight experience, to remove the possibility of flight experience causing changes in the brain of the bees that were sampled.

All bees were gently removed from the nest using large tweezers and then placed over ice to anaesthetise them before dissection. The entire heads of late larvae/pre-pupae and early-pupae were removed by cutting the anterior portion of the body by means of scissors ensuring that the whole head was included within the preparation and placed into 4% paraformaldehyde (PFA) in phosphate-buffered saline (PBS: 0.2562 g NaH<sub>2</sub>PO<sub>4</sub>·H<sub>2</sub>O, 1.495 g Na<sub>2</sub>HPO<sub>4</sub>·2H<sub>2</sub>O, 8.766 g NaCl per liter, pH 7.2–7.4) for fixation at 4 °C overnight. For mid-pupae, late pupae and adults, the heads were removed and the brains were immediately dissected out from the head capsule under cold 4% PFA in PBS. Subsequently, the brains of mid-pupae, late pupae and adults were put in fixative 4% PFA in PBS at 4 °C overnight. On the next day the tissue was washed in PBS three times (10 min each) before being transferred to 10% sucrose/PBS and 20% sucrose/PBS for 4 h each at room temperature and 30% sucrose/PBS overnight at 4 °C for cryoprotection. On the next day, the tissue was embedded in optimal cutting temperature compound (O.C.T.; Agar Scientific Ltd, UK) and rapidly frozen on dry ice before being sectioned into 10 μm slices. Serial brain sections were

alternately mounted onto positively charged SuperFrost Ultra Plus slides for later use (Fisher Scientific UK Ltd).

## 2.2. Probe synthesis

*In situ* hybridisation of bumblebee brain cryosections was conducted with digoxigenin (DIG)-labeled riboprobes. For *PRMT1*, antisense and sense probes were transcribed from a pBluescript II SK (+/–) subclone containing a 575-bp fragment from the coding DNA sequence (CDS) region (bp 539–1113; NCBI RefSeq: XM\_003395460.2) of the *PRMT1* cDNA. DNA containing the *PRMT1* fragment flanked by T3 RNA polymerase and T7 RNA polymerase sites was amplified by PCR. The antisense probe was synthesised using T3 RNA polymerase, whereas the sense probe was synthesised using T7 RNA polymerase. For *PRMT4/CARMER*, antisense and sense probes were transcribed from a pcDNA3 subclone containing a 517-bp fragment from the 3'-untranslated region (bp 2364–2880; NCBI RefSeq: XM\_012313193.1) of the *PRMT4* cDNA. DNA containing the *PRMT4* fragment flanked by SP6 RNA polymerase and T7 RNA polymerase sites was amplified by PCR. The antisense probe was synthesised using SP6 RNA polymerase, whereas the sense probe was synthesised using T7 RNA polymerase. For *PRMT5*, antisense and sense probes were synthesised from a 463-bp fragment from the CDS region (bp 1626–2088; NCBI RefSeq: XM\_003396560.2) of the *PRMT5* cDNA pcDNA3 clone. DNA containing the *PRMT5* fragment flanked by SP6 RNA polymerase and T7 RNA polymerase sites was amplified by PCR. The antisense probe was synthesised using SP6 RNA polymerase with a PCR amplified fragment from the plasmid, whereas the sense probe was synthesised using T7 RNA polymerase. A DIG RNA Labeling Kit (Roche, UK) was used to synthesise the DIG-labeled riboprobes according to the manufacturer's instructions.

## 2.3. *In situ* hybridisation (ISH)

Frozen horizontal brain sections were air dried for two hours and then washed twice for 7 min in PBS before being post-fixed in 4% PFA at room temperature for 20 min. This was followed by three 5-minute washes with PBS containing 0.1% Tween20 (Sigma-Aldrich, UK) (PBST). Slides were then incubated at 37 °C for 7 min in 20 mg/mL Proteinase K (Roche, UK) in Tris/EDTA (6.25 mM EDTA, 50 mM Tris, pH 7.5) to increase probe penetration and then were put into 4% PFA for 5 min to prevent the sections from falling apart. The sections were then washed in PBST three times (5 min per time), and acetylated in an acetylate solution (0.1 M Triethanolamine (TEA), 0.25% acetic anhydride, 0.175% acetic acid) for 10 min in order to remove the charge on the sections and eliminate the background binding of the probes later. This was followed by two 5-minute PBST washes and one 5-minute wash in 5 × saline sodium citrate (SSC; Na-citrate 0.075 M, NaCl 0.75 M, pH 7). Sections were then incubated in pre-hybridisation buffer (50 µg/mL yeast RNA, 50% Formamide, 20% 20 × SSC, 50 µg/mL Heparin and 0.1% Tween 20) for two hours at room temperature. Subsequently, hybridisation was performed by incubating the sections overnight at 65 °C with hybridisation buffer, which contained a DIG-labeled *ribo*-probe of either antisense or sense of *PRMT1*, 4 and 5 at a concentration of 1 µg/mL. On the following day, slides were equilibrated in 5 × SSC once for 20 min and 0.2 × SSC for 40 min twice at 65 °C. This was followed by a 10 min 0.2 × SSC wash and a 10-minute buffer B1 (5 M NaCl, 1 M Tris, pH 7.5) wash at room temperature. Slides were then blocked in buffer B1 with 5% goat serum for two hours at room temperature, and incubated with Anti-Digoxigenin-AP Fab Fragments (Roche, UK) antibody diluted 1:3000 in buffer B1 with 2.5% goat serum overnight at 4 °C. On the next day, the slides were washed with buffer B1 three times and once with buffer B3 (1 M MgCl<sub>2</sub>, 5 M NaCl and 1 M Tris, pH 9.5). Products were visualised using NBT/BCIP reagent (Roche, UK) according to the manufacturer's instructions in buffer B3 with 0.1% of Tween 20 (Sigma-Aldrich, UK) in a dark and humidified chamber. The staining was detected by the presence of dark

purple precipitate. Conditions for colour development were kept identical for all experiments performed with each sense and antisense probe. Colour development was monitored by using a LEICA DMR4 microscope (LEICA, Germany) every half an hour to determine when to stop the reaction. Reactions were stopped by putting the slides in deionised water when a moderate intensity of staining was achieved.

Slides were then mounted. For the mounting procedure, the slides were washed with deionised water three times (5 min each), and subsequently dried for about 45 min at 37 °C until they were totally dry before being put in 100% ethanol to dehydrate twice for 10 s, and equilibrated in histo-clear (National Diagnostics, UK) twice (7 min each). Histo-mount (National Diagnostics, UK) was then added to the slides before cover slips were added. Following this, the slides were allowed to dry and stored in a dark box.

Sections were photographed with a QIMAGING QIClick™ CCD Colour Camera linked to a DMRA2 light microscope (LEICA, Germany) using image analysis software (Volocity® software, v.6.3.1, PerkinElmer, USA) running on an iMac (27-inch, Version 10.10, Late 2013 model with OS X Yosemite). Photographs of half brain sections were collected (the other half of the brain showed symmetrical staining). Adjacent sections from the same brain were used for sense and antisense probes to ensure the specificity of the staining with antisense probes.

## 2.4. Quantification of ISH data for *PRMT1*

To quantify relative intensities of mRNA expression, ImageJ was used to determine the optical density of selected regions as a measure of gene expression (Schindelin et al., 2012). Thirty areas from the mushroom bodies, optic lobes, antennal lobes and background (no *PRMT1* ISH staining) neuropil areas were chosen for analysis. The goal was to choose areas that were from equivalent anatomical areas across the different sections and time-points. In Fig. 5A and B, areas 1–4 are the central mushroom bodies, areas 5–12 are the peripheral mushroom body, areas 13–18 are areas alongside the antennal lobe, and areas 19–24 are within the optic lobe area. In addition, a high intensity sub-region of the antennal lobe (area 13) was selected because in the early pupal stage this area repeatedly showed darker staining (we termed this the 'antennal lobe high intensity region'). Areas 25–30, within the neuropil region that lacked detectable staining, were chosen as the background areas. An example of the areas chosen are shown in Fig. 5A (original image of a bee section) and B (image showing the selected regions used for quantification). Areas high in noise (such as a folded section area or non-removable dirt on the cover slip) were avoided when choosing the areas of interest.

ImageJ was used to measure the optical density of the region of interest (ROI) (Schindelin et al., 2012). The average optical density of the background areas was subtracted from each ROI to normalise the intensity of the staining in each section. Five grouped areas (mushroom body central areas, mushroom body peripheral areas, antennal lobe high intensity area in early pupal stage, antennal lobe area and optic lobe area) were compared (see, for example, Fig. 5B).

## 2.5. Immunohistochemistry

Tissue sections which were hybridised with a *PRMT1* specific antisense riboprobe were then used for immunohistochemistry. All cell nuclei were detected using the DNA binding Hoechst stain, which allowed us to quantify the total number of cells. Mitotically-active cells were detected using anti-phospho-Histone H3 Serine 10 antibody. The slides were washed with PBS and blocked in 5% bovine serum albumin (BSA; Sigma-Aldrich, UK)/PBS-0.1% Triton X-100 (Sigma-Aldrich, UK) (PBS-Tx containing 5% BSA) at room temperature for 1 h, and incubated with 5% BSA/PBS-Tx containing 1:500-fold diluted anti-Phospho-Histone H3 [pSer10] antibody (PH3S10; produced in rabbit; Sigma-Aldrich, UK) at 4 °C overnight. The next day the slides were

washed three times in PBS (10 min for each wash) and incubated with a Cy2-conjugated anti-rabbit IgG secondary antibody at 1:500 dilution (Jackson ImmunoResearch, UK) and Hoechst 33,258 (1 µg/ml; Sigma-Aldrich, UK) for 2 h. This was followed by three washes with PBS-Tx (10 min each). Images were analysed using a fluorescence microscope (LEICA DMRA2, LEICA, Germany) and photographed with a digital camera (HAMAMATSU, ORCA-ER, C 4742–80, HAMAMATSU, Japan). The photographs were saved in Volocity software (v.6.3.1, PerkinElmer, USA) running on an iMac (27-inch, Version 10.10, Late 2013 model with OS X Yosemite, Apple, USA).

### 2.6. Correlation analysis of *PRMT1* expression with mitotically-active cells and cell density within mushroom bodies

The optical density of staining associated *PRMT1* mRNA expression was compared with the proportion of mitotically active cells measured as the number of anti-PH3S10 positive nuclei divided by the total number of nuclei (identified by Hoechst staining) in each selected region of the mushroom bodies.

To do this, the ISH image was used to select five ROIs in the dark stained region (central region) of the mushroom body and five ROIs in the left and right-side regions (peripheral regions) of the mushroom body to analyse. Two regions of background in the non-stained neuropil were also chosen to normalise the optical density of ISH image. The ISH channel was used to select these regions to avoid any bias involved in selecting the mitotic marker stained regions. The optical density of each selected region and the region size were measured using Fiji ImageJ software (Schindelin et al., 2012). The corresponding numbers of nuclei stained with Hoechst and numbers of PH3S10-expressing cells in the same selected regions were counted. An example of how ROIs were selected is shown in Supplemental Fig. S2.

Spearman's rank correlation coefficient analysis was used to analyse the correlation between the expression level of *PRMT1* (measured as optical density normalised by the subtraction of the background optical density) and proportion of mitotically active cells (the number of PH3S10-positive dividing nuclei divided by the total number of nuclei) in each selected region for three developmental stages of bumblebees (late larvae/pre-pupae, early-pupae and mid-pupae).

Furthermore, the Hoechst stained image and the ISH image was analysed to gain a better understanding of the relationship between the cell density (measured as the number of nuclei divided by the size of the area) and the expression level of *PRMT1* in the same region. Spearman's rank correlation coefficient analysis was also used to determine whether there is a spatio-temporal correlation between *PRMT1* mRNA expression level and the cell density during the three stages of bumblebee development. R statistical software version 3.4.0 was used in the analyses above (R Core Team, 2017).

## 3. Results

### 3.1. *In situ* hybridisation analysis of *PRMT* gene expression in pupal and adult bumblebee brains

To gain insights into potential roles of PRMTs in bumblebee neural development, we performed *in situ* hybridisation to determine the mRNA expression pattern of *PRMT1*, *PRMT4* and *PRMT5* in the developing brain of bumblebees. We selected the late larval/pre-pupal, early-pupal, mid-pupal, late pupal, two-day old worker, and 7–10-day old worker stages to investigate mRNA expression of *PRMT1*, 4 and 5, since the first three developmental stages are marked by active neurogenesis in the mushroom body, while it ceases after the mid-pupal stage (Farris et al., 1999).

Our results show that all three genes are expressed throughout pupal development and adult stages in cell bodies of neural precursors and nerve cells in the mushroom bodies, antennal lobes, and optic lobes (Figs. 2–4 and sense controls in Supplementary Fig. S3–S5).

Interestingly, we observed that the expression of all PRMTs was more uniform in level in the adult brain (Figs. 2–4D–F) compared to the localised elevated expression of specific PRMT mRNAs seen in the pupal brain (Figs. 2–4A–C), suggesting a role for these enzymes in pupal brain development.

### 3.2. *PRMT1* mRNA expression

Visual inspection of sections from the late larvae/pre-pupae, early-pupae and mid-pupae developmental stages revealed that the expression level of *PRMT1* mRNA was higher in the mushroom body central regions, which are thought to contain dividing neural precursors (arrows in Fig. 2), than in the mushroom body peripheral regions, which are thought to contain differentiated neurons, at least in honeybees (Fig. 2A–C) (Farris et al., 1999; Kurshan et al., 2003). Previous studies in honeybees have shown that neuroblast clusters localise at the central region of mushroom bodies where they divide before they differentiate and migrate to the periphery of the neuroblast clusters (Farris et al., 1999; Kurshan et al., 2003). The newly born post-mitotic neurons, called Kenyon cells, are located at the periphery of the neuroblast clusters (Farris et al., 1999; Kurshan et al., 2003). The stronger localised expression of *PRMT1* mRNA in central mushroom body areas during earlier stages of development contrasted with its uniform expression pattern in the late pupal and adult stages (Fig. 2D, E and F). There were no clear differences in expression in sections from two-day old workers and 7–10-day old workers.

### 3.3. *PRMT4* and *PRMT5* mRNA expression

In contrast to *PRMT1*, *PRMT4* and *PRMT5* mRNAs were more uniformly expressed across all stages (Figs. 3 and 4) except for the early pupal stage (Figs. 3B and 4B). There was a slightly higher expression level of *PRMT4* and *PRMT5* in central mushroom bodies at early pupal stage (Figs. 3B and 4B), although this was less distinct than the markedly elevated level of expression observed for *PRMT1*. No clear differences in expression levels of either *PRMT4* or 5 were detected in any of the sub-regions of the mushroom bodies, optic lobes or antennal lobes at other developmental stages investigated (*PRMT4*: Fig. 3A and C–F, *PRMT5*: Fig. 4A and C–F).

### 3.4. Quantification of relative *PRMT1* mRNA expression

We noticed that *PRMT1* mRNA was preferentially expressed in the central mushroom body regions in pre-, early and mid-pupal stages (Fig. 2A–C), at the time when neurogenesis occurs in the honeybee (Farris et al., 1999). Given the importance of central mushroom bodies for neuroblast/ganglion mother cell divisions we sought to quantify the relative expression level of *PRMT1* mRNA within different selected regions of the CNS. To this end, we measured the optical density of 24 areas of the CNS grouped into 4 anatomical regions (Fig. 5A and B and see also Materials and Methods). For the early pupal stage we observed an additional high intensity sub-region of the antennal lobe, which was also selected for analysis. The results are shown in Fig. 5C. *PRMT1* expression was higher in the central mushroom body areas, and a sub area of the antennal lobe, than in other areas during the late larvae/pre-pupae, early pupae and mid-pupae developmental stages. The higher *PRMT1* mRNA expression level within these areas of mushroom bodies and antennal lobe during these developmental stages suggests that there may be a functional significance for high PRMT1 levels during these stages of the mushroom bodies and antennal lobes development. The antennal lobes are the principal neural relay of olfactory processing in insects, functionally equivalent to the vertebrate olfactory bulb (Hansson and Anton, 2000). The mushroom bodies are sensory integration centres which review information from the antennal lobes (Hansson and Anton, 2000). The specific functional significance of the high-intensity sub-region of the antennal lobe that we identified in the

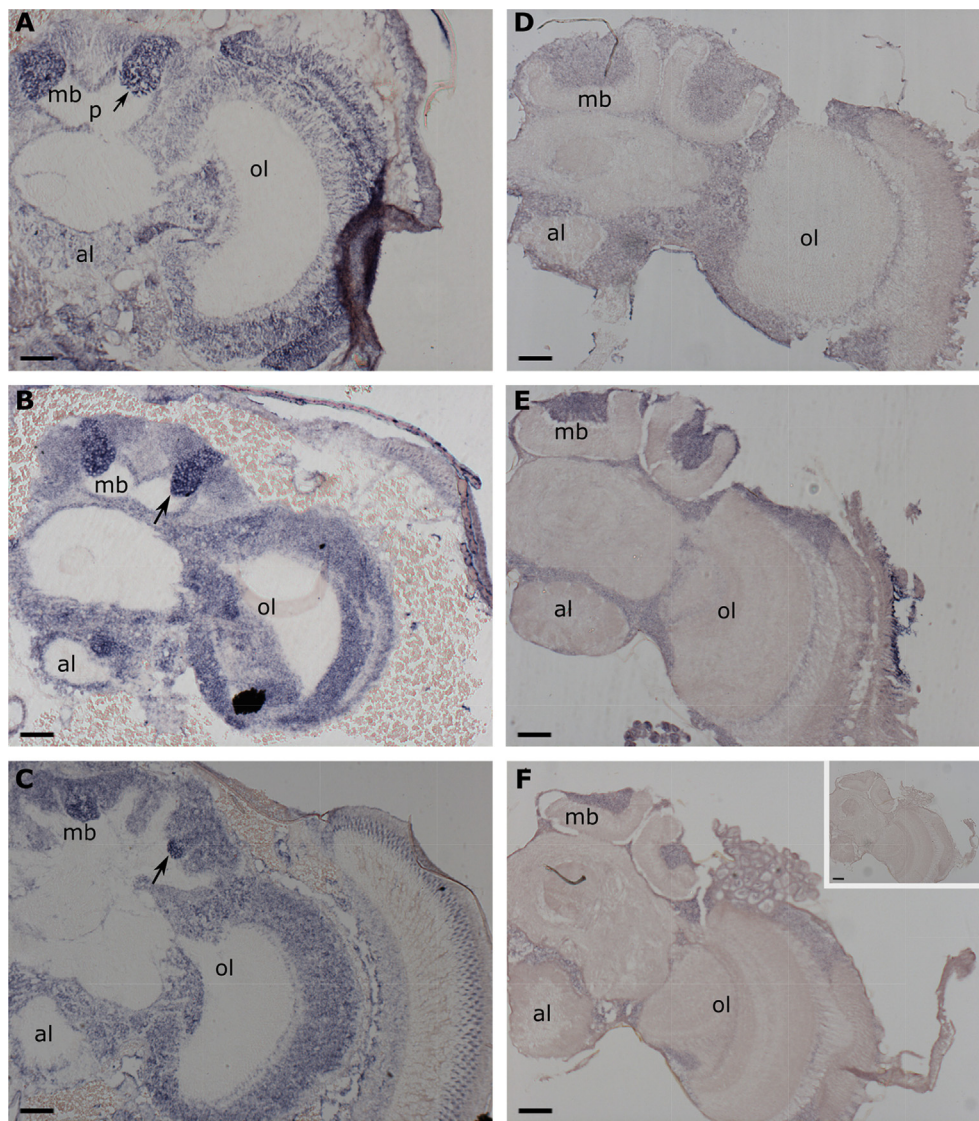


**Fig. 2.** *In situ* hybridisation of *PRMT1* in the frontal half section of the brain of A) late larva/pre-pupa; B) early pupa; C) mid-pupa; D) late pupa; E) two-day old worker and F) 7–10-day old worker. Three biological replicates were analysed for each stage. Arrow: neural precursor dividing regions according to honeybee literature. mb: mushroom body; ol: optic lobe; al: antennal lobe; p: pedunculus. F) inset panel shows sense control without signal. Scale bars: 120  $\mu$ m.

early pupal stage is unclear at this stage.

### 3.5. High levels of *PRMT1* expression are found in areas of mitotically active cells within the mushroom bodies

*PRMT1* was preferentially expressed in the centre of the mushroom bodies, the area which is recognised as a region containing dividing neuroblasts and ganglion mother cells from larval to mid-pupal stages in honeybees (Farris et al., 1999; Kurshan et al., 2003; Malun, 1998). Therefore, we investigated whether the same anatomical areas also contain dividing cells in bumblebees. To this end, we used an antibody that marks mitotically active cells to co-immunolabel sections of the bumblebee brains used for ISH analysis of *PRMT1* mRNA expression to determine if higher levels of *PRMT1* mRNA correlate with the prevalence of mitotically active cells. The antibody against phosphorylated serine 10 on histone H3 (PH3S10) is specific for the metaphase and anaphase stages of mitotically active cells (Giet and Glover, 2001). We found that sub-regions of the mushroom bodies of the late larva/pre-pupa, early pupa, and mid-pupa that expressed high levels of *PRMT1* mRNA as detected by ISH, also contained a number of mitotically active cells (Fig. 6M–O). The observed number of mitotically active cells is

likely to underestimate the total number of dividing cells because PH3S10 only marks the metaphase and anaphase stages of the cell cycle (Giet and Glover, 2001).

In contrast, in late pupal and adult stages, there was a more uniform expression pattern of *PRMT1*, and we did not detect any cells expressing PH3S10 (Supplementary Fig. S6). Equivalent images of pupal stages captured using identical imaging settings are shown for comparison to demonstrate that mitotically-active PH3S10 positive cells are visible at the same magnification (Supplementary Fig. S6). These observations suggest that there were no dividing cells in the adult brain, consistent with previous observations that demonstrated the absence of adult neurogenesis in honeybees (Fahrbach et al., 1995; Farris et al., 1999; Kurshan et al., 2003).

### 3.6. Higher *PRMT1* expression correlates with mitotically active cells and lower cell density in the mushroom bodies

We quantified the relationship between higher expression of *PRMT1* and the prevalence of mitotically active cells (detected by PH3S10 immunoreactivity) within the central sub-regions of mushroom body areas in late larvae/pre-pupae, early pupae and mid-pupae. Spearman's

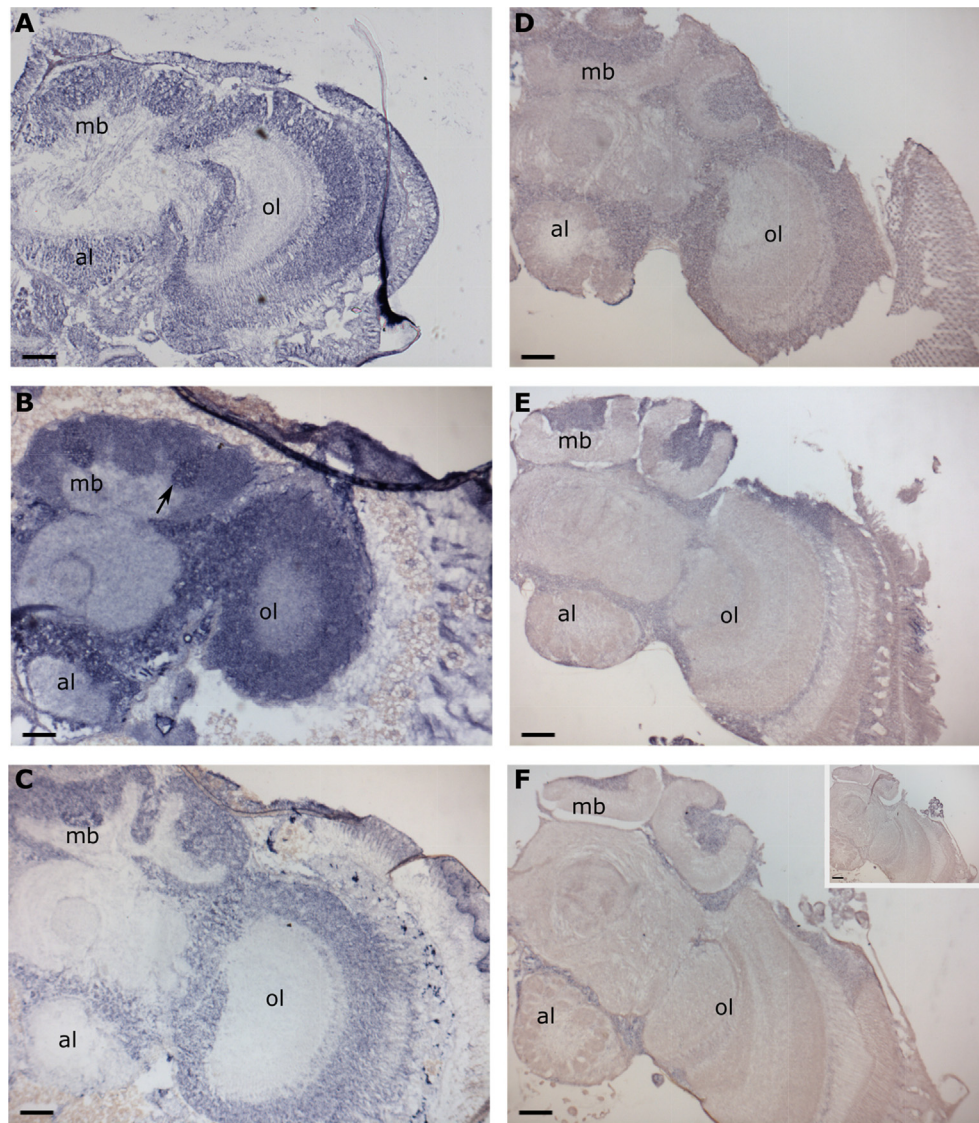


**Fig. 3.** *In situ* hybridisation of *PRMT4* in the frontal half section of the brain of A) late larva/pre-pupa; B) early pupa; C) mid-pupa; D) late pupa; E) two-day old worker and F) 7–10-day old worker. Three biological replicates were analysed for each stage. Arrow: higher expression region. mb: mushroom body; ol: optic lobe; al: antennal lobe. F) inset panel shows sense control without signal. Scale bars: 120  $\mu$ m.

rank correlation coefficient was used to investigate the correlation between the expression level of *PRMT1* and the proportion of mitotically active cells (the number of PH3S10 expressing cells divided by the total number of cells as determined by the number of nuclei labelled with Hoechst) for each stage. Results presented in Fig. 7B and C showed that there was a positive correlation (Fig. 7B:  $\rho = 0.46$ ,  $df = 43$ ,  $p$ -value = 0.0015; C:  $\rho = 0.46$ ,  $df = 43$ ,  $p$ -value = 0.0015) between the proportion of mitotically active cells within a region and the level of *PRMT1* expression in that region of mushroom bodies during early and mid-pupal stages. The correlation in late larval/pre-pupal stage was weaker and not significant (Fig. 7A:  $\rho = 0.22$ ,  $df = 43$ ,  $p$ -value = 0.14), although the co-immunolabelling of *PRMT1* ISH and PH3S10 immunohistochemistry (Fig. 6M) showed that many PH3S10 positive cells were within or close to the stronger *PRMT1* ISH signal region in the central mushroom body area, but were less restricted to the higher *PRMT1* ISH signal region than in the early- and mid-pupal stages.

These results show that in the central mushroom body areas, at least during the early- and mid-pupal stages, high levels of *PRMT1* expression are spatially-associated with increased mitotic activity.

In analysing Hoechst stained images, we noticed that there were fewer nuclei in the central region of the mushroom bodies than in the

outer regions of the mushroom bodies (Fig. 6G–I). In order to confirm this observation, we analysed and quantified the cell density in each region of interest. Results from Fig. 7D–F demonstrate that regions which show higher expression of *PRMT1* within the mushroom bodies correlated with the regions showing lower cell density (late larvae/pre-pupae/D:  $\rho = -0.37$ ,  $df = 43$ ,  $p$ -value = 0.013; early pupae/E:  $\rho = -0.4$ ,  $df = 43$ ,  $p$ -value = 0.0056; mid-pupae/F:  $\rho = -0.57$ ,  $df = 43$ ,  $p$ -value =  $5.9 \times 10^{-5}$ ). It is well documented that neuroblasts in the honeybee and *Drosophila* have bigger cell bodies than differentiated neurons, which may account for a lower cell density in the areas of mitotic activity (Farris et al., 1999; Homem et al., 2014; Siegrist et al., 2010). We have already shown that regions containing high *PRMT1* expression are associated with mitotically active cells. Our observation that the cell density is reduced within this part of MB further suggests that this region probably contains dividing neuroblasts (Farris et al., 1999; Kurshan et al., 2003; Malun, 1998).

#### 4. Discussion

In the present study, we began to investigate the roles of PRMTs in the CNS development of bumblebees by analysing the expression

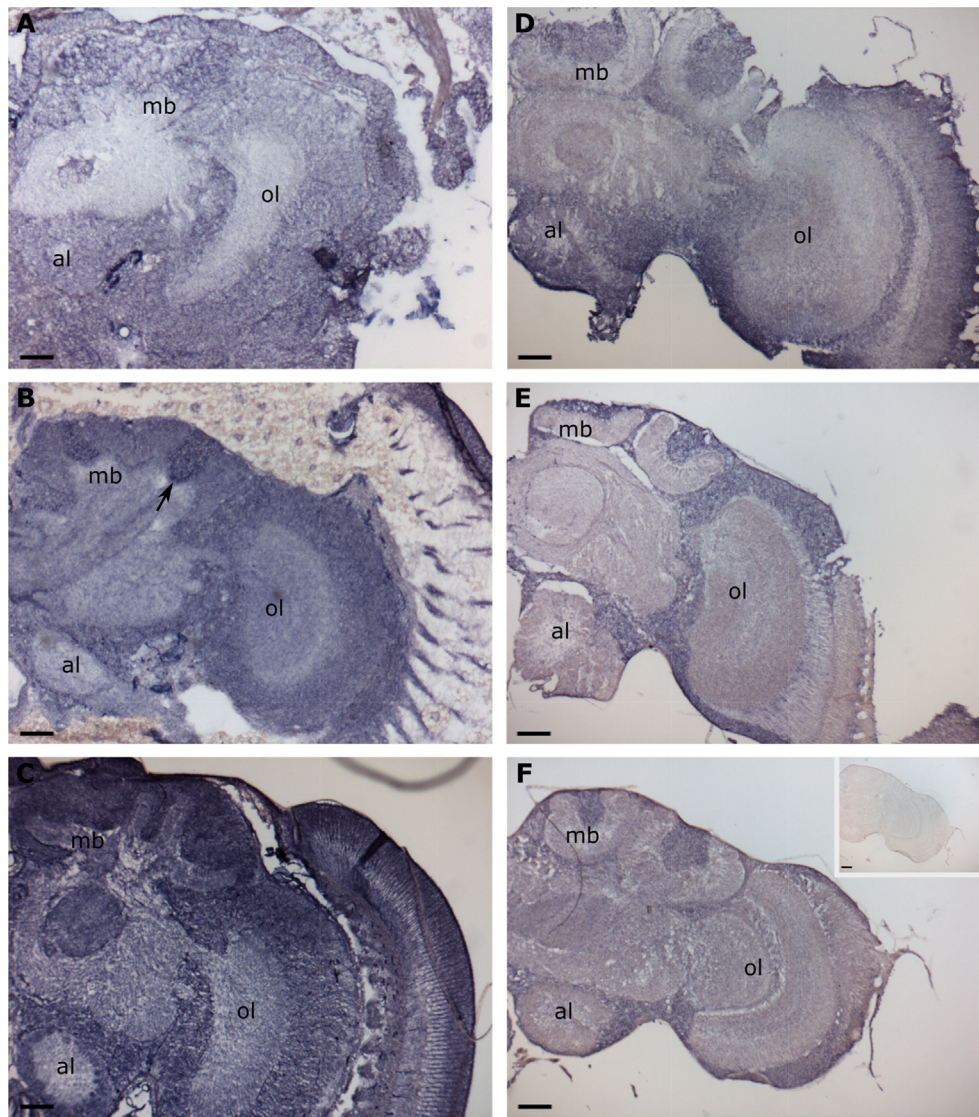


**Fig. 4.** *In situ* hybridisation of *PRMT5* in the frontal half section of the brain of A) late larva/pre-pupa; B) early pupa; C) mid-pupa; D) late pupa; E) two-day old worker and F) 7–10-day old worker. Three biological replicates were analysed for each stage. Arrow: higher expression region. mb: mushroom body; ol: optic lobe; al: antennal lobe. F) inset panel shows sense control without signal. Scale bars: 120  $\mu$ m.

pattern of several *PRMT* genes in the developing brain of these insects. We found that all three *PRMTs* investigated are expressed in the developing CNS of bumblebees. The widespread expression of these genes in bumblebee brains at all developmental stages investigated suggests that they may be important throughout the life cycle of the bumblebee. Previous research into the function of *PRMTs* in several model organisms highlighted the multitude of processes controlled by these enzymes, such as regulation of RNA processing, DNA damage repair and signal transduction, but also their important roles in the control of neural stem cell (NSC) proliferation and homeostasis, both during development and in the adult (Bedford and Clarke, 2009; Bezzi et al., 2013; Blackwell and Ceman, 2012; Blanc and Richard, 2017). The uniform expression of *PRMTs* in the adult brain may be indicative of their primary involvement in maintaining tissue homeostasis in the adult brain, rather than being involved in specifically localised processes such as proliferation and differentiation of precursor cells occurring during development. Our findings that the *PRMTs* are expressed throughout the life cycle of bumblebees are thus consistent with the observations from other model organisms.

Interestingly, we found that *PRMT1* was particularly highly expressed in the central mushroom body regions, which have been

identified in honeybees as regions containing dividing neuroblasts/ganglion mother cells. Whilst it is not certain that areas of high *PRMT1* expression levels in the bumblebee also contain dividing neuroblasts/ganglion mother cells, such a possibility is plausible and supported by the observation that high levels of *PRMT1* expression show significant spatial correlation with the mitotic marker, PH3S10, during early and mid-pupal stages. Moreover, we observed that higher levels of *PRMT1* expression within the central mushroom body showed significant spatial correlation with regions of lower cell density. Neuroblasts in the honeybee and *Drosophila* have bigger cell bodies than differentiated neurons, which may account for the lower cell density we observed in the areas of high *PRMT1* expression characterised by the presence of mitotic activity (Farris et al., 1999; Homem et al., 2014; Siegrist et al., 2010).

These observations are intriguing given the developmental programmes taking place within the bumblebee mushroom bodies during these stages. While there is very little information about these processes in bumblebees, more is known about the developmental fates of neuroblasts in the mushroom bodies of honeybees and in *Drosophila*. Larval development in honeybees is characterised by an increase in neuroblast numbers initially, with ganglion mother cells and Kenyon cells being

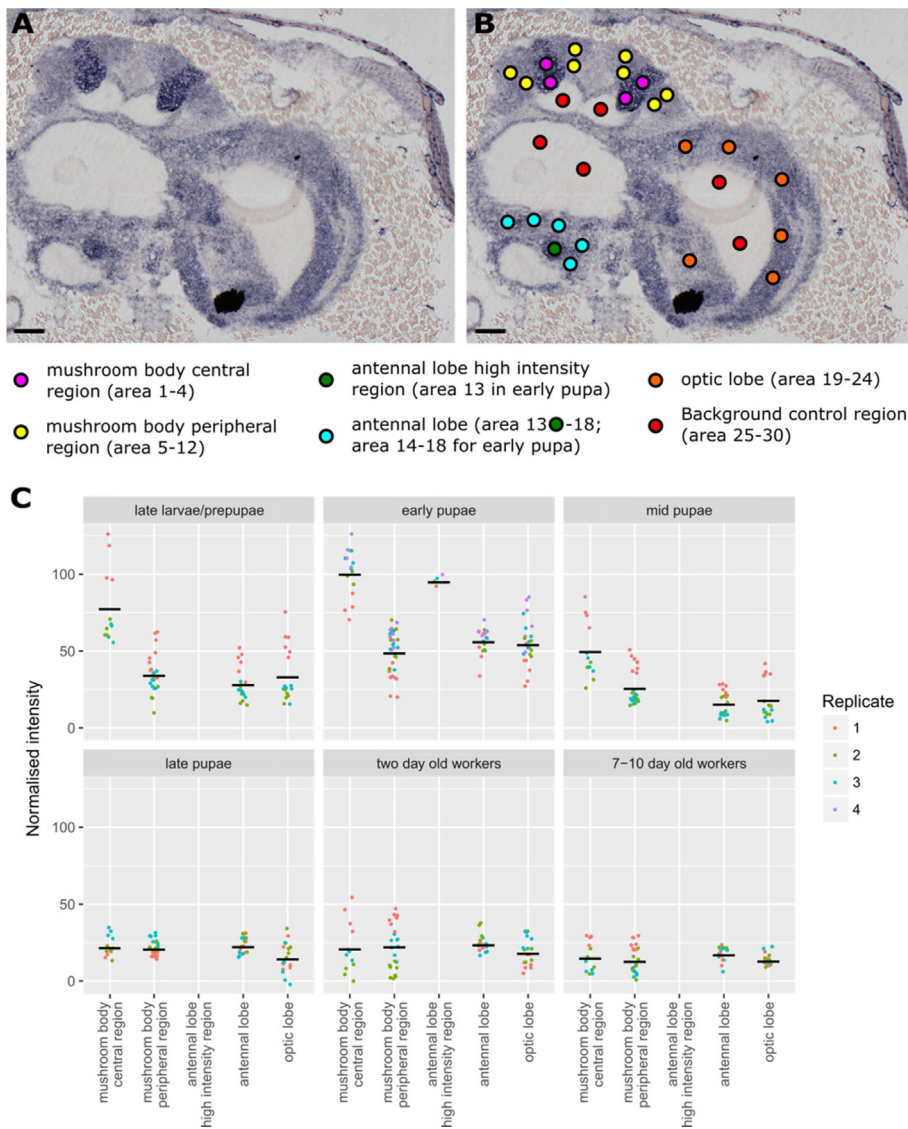


**Fig. 5.** Quantification of the relative expression levels of *PRMT1* mRNA in selected areas of brains at different stages of development. A) An image example of ISH of *PRMT1* in early pupal bumblebee brain. B) Same image as in A) showing how the sub-regions to be analysed were grouped into four or five anatomical areas. C) Graph showing levels of *PRMT1* expression in brain areas (mushroom body central area, mushroom body peripheral area, antennal lobe high intensity area in early pupal stage, antennal lobe area and optic lobe area) at different stages of development. The dots indicate relative expression levels of *PRMT1*. There were three biological replicates for every stage, except for the early pupae stage where there were four biological replicates. For each stage of development six sub-regions (blue and green dots shown in B) were analysed in the antennal lobe apart from early pupal stage (five sub-regions). In early pupa, a high intensity sub-region of antennal lobe was also chosen and analysed. Different biological replicates are marked with differently coloured dots in each developmental stage. The same colour of dots in each stage were from the same individual bee. The mean of each grouped area is signified by the black bars. Scale bars: 120  $\mu$ m.

born towards the later larval stages until mid-late pupal stages (Farris et al., 1999). It is noteworthy in this respect that in our study we found that in the late larval/pre-pupal stage the correlation between the level of *PRMT1* expression and the number of mitotic cells was weak, while it became stronger during the early- and mid-pupal stages. These stages correspond to two developmental events in the honeybee (Farris et al., 1999). Firstly, during the late-larval stage the neuroblast and ganglion mother cell numbers remain high as Kenyon cells are born, suggesting a balance between proliferative and neurogenic divisions. Secondly during the early- and mid-pupal stages neuroblast and ganglion mother cell numbers decrease, whilst Kenyon cells rapidly increase in number, suggesting that neurogenic divisions predominate (See Fig. 1B) (Farris et al., 1999). Later in development, from the mid-late pupal stage, the neuroblasts are removed by apoptosis and neurogenesis stops (Farris et al., 1999).

These observations suggest that high levels of *PRMT1* may favour neurogenic divisions of neuroblasts and ganglion mother cells to generate ganglion mother cells and Kenyon cells, respectively. This idea is further supported by the observations of mammalian cortical development, where neural stem cells that are undergoing neurogenic division to either generate intermediate basal progenitors (IBPs) or IBPs dividing to generate two neurons express high levels of the anti-proliferative gene *TIS21/BTG2*, that stimulates the activity of *PRMT1* (Canzoniere et al., 2004; Haubensak et al., 2004; Iacopetti et al., 1999).

Importantly, a *TIS21* orthologue is also present in bumblebees (accession number: LOC100648380; *BTG2*). Thus, the *TIS21/PRMT1* axis may form part of a general mechanism controlling neurogenic divisions during development of a variety of animal species. It will be important to probe this possibility further in future studies.

In the present study we did not detect any mitotically-active cells in the late pupae and adult stages, suggesting that in the mushroom bodies of bumblebees, neurogenesis ceases during pupal development. These observations align well with previous work in honeybees, which showed that developmental neurogenesis ceases in the mushroom bodies after the mid-pupal stage, as manifested by an absence of detectable mitotically-active neuroblasts and ganglion mother cells (Farris et al., 1999; Kurshan et al., 2003; Malun, 1998; Roat and da Cruz Landim, 2010). We cannot, however, fully exclude the possibility that adult neurogenesis may occur in bumblebees in particular situations such as brain damage as it has been observed in other insects. For example, in crickets (*Acheta domesticus*), neurogenesis in mushroom body also takes place in the adult (Cayre et al., 1994). In addition, acute brain damage to the *Drosophila* medulla cortex triggers adult neurogenesis (Fernández-Hernández et al., 2013). In contrast to the lack of adult neurogenesis in honeybees, changes in neural morphology and connectivity do occur. Foraging honeybees have more dendritic spines in the mushroom body in comparison to nursing bees, which are normally younger than foraging bees (Durst et al., 1994; Fahrbach et al.,

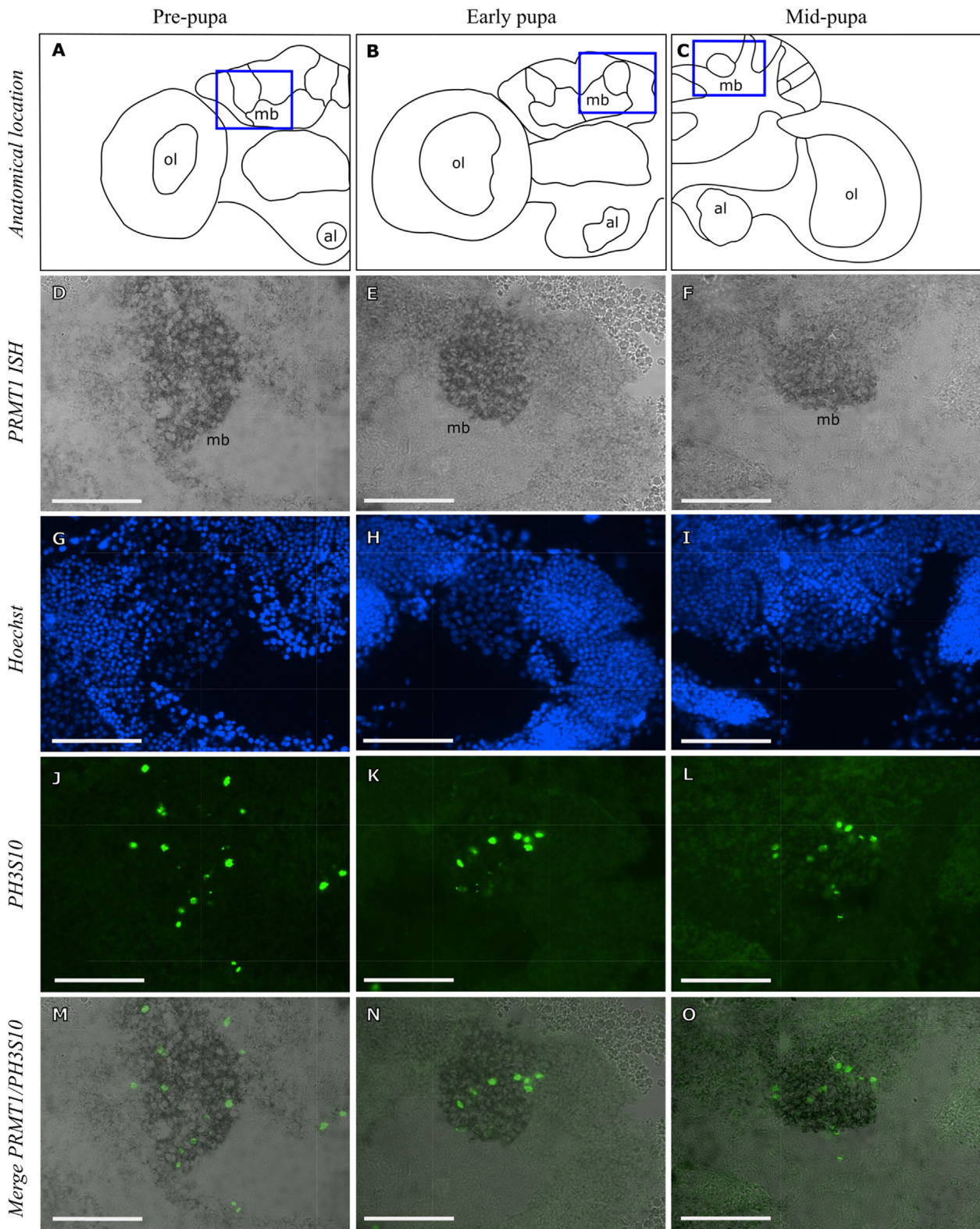


**Fig. 6.** Areas of high *PRMT1* mRNA expression are enriched for dividing cells in the late larval/pre-pupal, early pupal and mid-pupal brain. A–C) Schematic diagrams of the late larval/pre-pupal, early pupal and mid-pupal brains showing the anatomical location of the mushroom bodies analysed in this study. D–F) *In situ* hybridisation of *PRMT1* in the late larval/pre-pupal, early pupal and mid-pupal mushroom bodies. G–I) Hoechst detection of all nuclei in the late larval/pre-pupal, early pupal and mid-pupal mushroom bodies. J–L) Immunohistochemical detection of mitotically active cells with anti-phospho-histone H3 Ser 10 antibody in the late larval/pre-pupal, early pupal and mid-pupal mushroom bodies. M–O) Merged image of *PRMT1* expression and phospho-histone H3 Ser 10 immunoreactivity in the late larval/pre-pupal, early pupal and mid-pupal mushroom bodies. mb: mushroom body; ol: optic lobe; al: antennal lobe. Boxes indicate the anatomic location of the mushroom bodies analysed in this study. Scale bars: 100 μm.

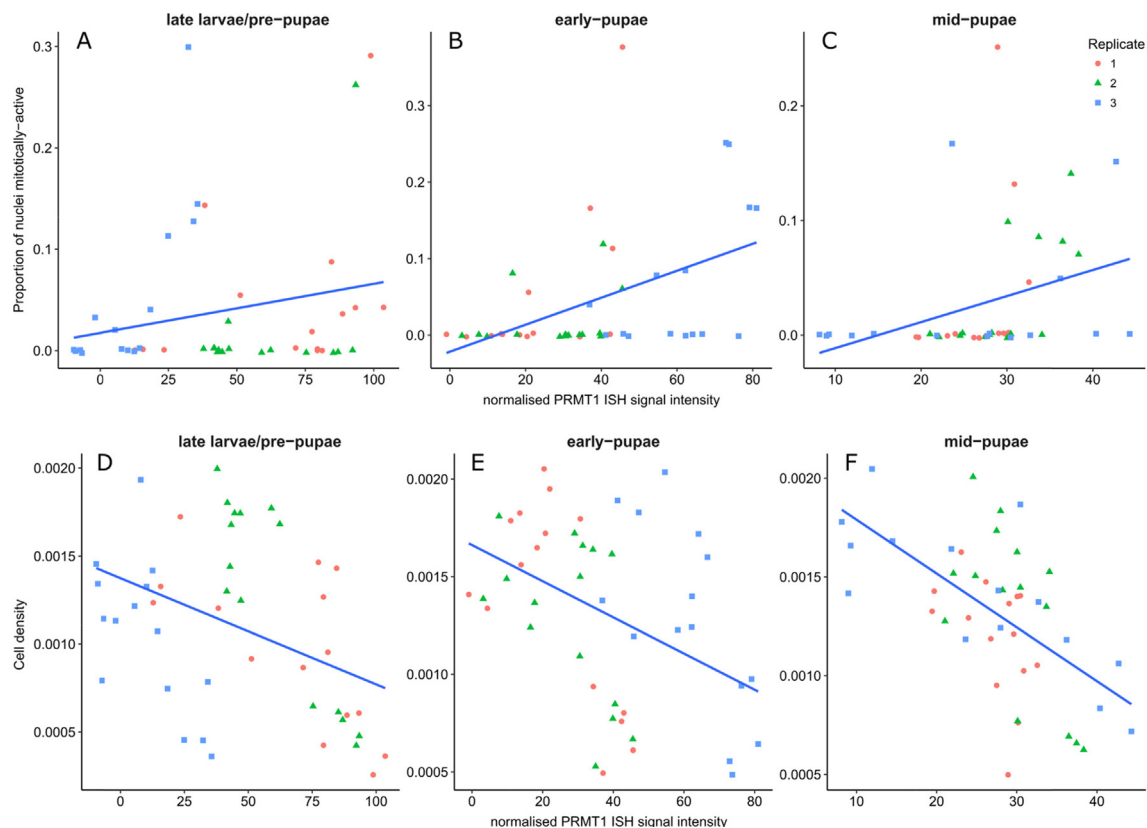


**Fig. 7.** Correlation analysis of *PRMT1* expression levels and PH3S10 positive cells and cell density. A–C) Correlation between the normalised optical density of *PRMT1* ISH signals (X axis) and proportion of mitotically active cells (the number of PH3S10 expressing cells divided by the total number of cells as determined by the number of nuclei labelled with Hoechst, Y axis) in each selected region for three different stages of bees. A) 3 late larvae/pre-pupae, B) 3 early pupae and C) 3 mid-pupae. There is a moderately significant correlation between the higher proportion of dividing cells and higher expressed level of *PRMT1* for B) early pupae,  $\rho = 0.46$ ,  $df = 43$ ,  $p$ -value = 0.0015 and C) mid-pupae,  $\rho = 0.46$ ,  $df = 43$ ,  $p$ -value = 0.0015. There is no significant correlation for A) late larvae/pre-pupae,  $\rho = 0.22$ ,  $df = 43$ ,  $p$ -value = 0.14. The dots which are close to 0 value on the Y axis indicate that in these selected regions, there are no PH3S10 expressing cells. D–F) Correlation between the normalised optical density of *PRMT1* ISH signals (X axis) and cell density (total number of Hoechst stained nuclei divided by the size of the region, Y axis) in each selected region for three different stages of bees, D) 3 late larvae/pre-pupae, E) 3 early pupae and F) 3 mid-pupae. There is a stronger significant correlation between lower cell density with higher expressed level of *PRMT1* for all three developmental stages: D) late larvae/pre-pupae,  $\rho = -0.37$ ,  $df = 43$ ,  $p$ -value = 0.013; E) early pupae  $\rho = -0.4$ ,  $df = 43$ ,  $p$ -value = 0.0056; F) mid-pupae,  $\rho = -0.57$ ,  $df = 43$ ,  $p$ -value =  $5.9 \times 10^{-5}$ . Each dot corresponds to the values of each selected region. The blue line is best linear fit line.

1998; Farris et al., 2001; Groh et al., 2012). Neuropil growth of mushroom bodies occurs firstly during the time of the orientation flight of an adult honeybee and continues throughout its foraging life (Fahrbach et al., 1998), and foraging experience contributes to dendritic growth in the collar region (the visual input region) of the calyces of mushroom bodies (Dobrin et al., 2011; Groh et al., 2012).

The *PRMT4* and *PRMT5* *in situ* hybridisation results revealed a more uniform expression of both mRNAs at late larval/pre-pupal, mid- and late-pupal and adult stages. We observed a slightly stronger ISH signal in the proliferative regions of mushroom bodies in early-pupal stages for both *PRMT4* and *PRMT5* mRNAs. *PRMT4* induces PC12 cell (a cell line derived from a pheochromocytoma of the rat adrenal medulla) proliferation by methylating the RNA binding protein HuD, and inducing degradation of anti-proliferative *p21* mRNA bound by HuD (Fujiwara et al., 2006). *PRMT5* maintains proliferation of PC12 cells and mouse embryonic neural stem cells during early stages of development (Bezzi et al., 2013; Chittka, 2013; Chittka et al., 2012). *PRMT5* is also required for neural stem cell homeostasis, and its selective depletion in CNS in mice leads to CNS developmental defects and post-natal death within 14 days after birth (Bezzi et al., 2013). Furthermore, *PRMT5* expression is upregulated in solid tumors, lymphoma, and leukemia (Blanc and Richard, 2017). Together, these observations suggest that *PRMT4* and *PRMT5* may be required for maintaining cells in a proliferative state. It will be important to investigate whether *PRMT4* and *PRMT5* play a

similar role in the early pupal stage in bumblebees in the future. Functional molecular studies have historically been difficult in bumblebees due to lack of genetic tools such as mutants. However new CRISPR/Cas gene editing technology has recently been applied to insects including ants and honeybees (Kohno et al., 2016; Yan et al., 2017). The current work paves the way for such a functional study of *PRMT* function in bumblebees by defining the localisation and timing of *PRMT* gene expression in the brains of bumblebees.

## 5. Data accessibility

Raw data for Figs. 5 and 7 are provided in Supplementary Tables S1 and S2.

## Author contributions

CG, AC and LC conceived the study. CG, AC, CJP and LC designed the study; ME and AC provided technical support and advice for histology, mRNA *in situ* hybridisation, immunohistochemistry and photomicroscopy; CG performed experiments; CG and CJP analysed data; CG, AC, CJP and LC drafted the manuscript. All authors approved the manuscript.

## Competing interests

The authors declare that they have no competing interests.

## Funding

CG was supported by a studentship from the China Scholarship Council No. 201408360067, AC was supported by the BBSRC grant BB/J006602/1. LC received support from HFSP program grant (RGP0022/2014).

## Acknowledgments

We thank Maurice Elphick for providing access to research facilities in his laboratory and for providing feedback on the manuscript. We also thank Angelika Stollewerk, Petra Ungerer, Frederick Partridge, Thomas Butts and Weigang Cai for helpful discussions.

## Appendix A. Supplementary data

Supplementary data to this article can be found online at <https://doi.org/10.1016/j.jinsphys.2019.04.011>.

## References

- Batut, J., Vandel, L., Leclerc, C., Daguzan, C., Moreau, M., Néant, I., 2005. The Ca<sup>2+</sup>-induced methyltransferase xPRMT1b controls neural fate in amphibian embryo. *Proc. Natl. Acad. Sci. U.S.A.* 102, 15128–15133.
- Bedford, M.T., Clarke, S.G., 2009. Protein arginine methylation in mammals: who, what, and why. *Mol. Cell* 33, 1–13.
- Bezzi, M., Teo, S.X., Muller, J., Mok, W.C., Sahu, S.K., Vardy, L.A., Bonday, Z.Q., Guccione, E., 2013. Regulation of constitutive and alternative splicing by PRMT5 reveals a role for Mdm4 pre-mRNA in sensing defects in the spliceosomal machinery. *Genes Dev.* 27, 1903–1916.
- Blackwell, E., Ceman, S., 2012. Arginine methylation of RNA-binding proteins regulates cell function and differentiation. *Mol. Reprod. Dev.* 79, 163–175.
- Blanc, R.S., Richard, S., 2017. Arginine methylation: the coming of age. *Mol. Cell* 65, 8–24.
- Bullock, T., Horridge, G.A., 1965. *Structure and Function in the Nervous Systems of Invertebrates*.
- Canzoniere, D., Farioli-Vecchioli, S., Conti, F., Ciotti, M.T., Tata, A.M., Augusti-Tocco, G., Mattei, E., Lakshmana, M.K., Krizhanovsky, V., Reeves, S.A., 2004. Dual control of neurogenesis by PC3 through cell cycle inhibition and induction of Math1. *J. Neurosci.* 24, 3355–3369.
- Cayre, M., Strambi, C., Strambi, A., 1994. Neurogenesis in an adult insect brain and its hormonal control. *Nature* 368, 57.
- Chittka, A., 2013. Differential regulation of SCL/PRDM4 and PRMT5 mediated protein arginine methylation by the nerve growth factor and the epidermal growth factor in PC12 cells. *Neurosci. Lett.* 550, 87–92.
- Chittka, A., Nitaraska, J., Grazini, U., Richardson, W.D., 2012. Transcription factor positive regulatory domain 4 (PRDM4) recruits protein arginine methyltransferase 5 (PRMT5) to mediate histone arginine methylation and control neural stem cell proliferation and differentiation. *J. Biol. Chem.* 287, 42995–43006.
- Chittka, L., Niven, J., 2009. Are bigger brains better? *Curr. Biol.* 19, R995–R1008.
- Dobrin, S.E., Herlihy, J.D., Robinson, G.E., Fahrback, S.E., 2011. Muscarinic regulation of Kenyon cell dendritic arborizations in adult worker honey bees. *Arthropod Struct. Dev.* 40, 409–419.
- Durst, C., Eichmüller, S., Menzel, R., 1994. Development and experience lead to increased volume of subcompartments of the honeybee mushroom body. *Behav. Neural Biol.* 62, 259–263.
- Fahrback, S.E., Strande, J.L., Robinson, G.E., 1995. Neurogenesis is absent in the brains of adult honey bees and does not explain behavioral neuroplasticity. *Neurosci. Lett.* 197, 145–148.
- Fahrback, S.E., Moore, D., Capaldi, E.A., Farris, S.M., Robinson, G.E., 1998. Experience-expectant plasticity in the mushroom bodies of the honeybee. *Learn. Memory* 5, 115–123.
- Farris, S., Robinson, G., Davis, R., Fahrback, S., 1999. Larval and pupal development of the mushroom bodies in the honey bee, *Apis mellifera*. *J. Comp. Neurol.* 414, 97–113.
- Farris, S.M., Robinson, G.E., Fahrback, S.E., 2001. Experience-and age-related outgrowth of intrinsic neurons in the mushroom bodies of the adult worker honeybee. *J. Neurosci.* 21, 6395–6404.
- Fernández-Hernández, I., Rhiner, C., Moreno, E., 2013. Adult neurogenesis in *Drosophila*. *Cell Rep.* 3, 1857–1865.
- Fujiwara, T., Mori, Y., Chu, D.L., Koyama, Y., Miyata, S., Tanaka, H., Yachi, K., Kubo, T., Yoshikawa, H., Tohyama, M., 2006. CARM1 regulates proliferation of PC12 cells by methylating HuD. *Mol. Cell. Biol.* 26, 2273–2285.
- Ganeshina, O., Schäfer, S., Malun, D., 2000. Proliferation and programmed cell death of neuronal precursors in the mushroom bodies of the honeybee. *J. Comp. Neurol.* 417, 349–365.
- Giet, R., Glover, D.M., 2001. *Drosophila* aurora B kinase is required for histone H3 phosphorylation and condensin recruitment during chromosome condensation and to organize the central spindle during cytokinesis. *J. Cell Biol.* 152, 669–682.
- Greene, L.A., Tischler, A.S., 1976. Establishment of a noradrenergic clonal line of rat adrenal pheochromocytoma cells which respond to nerve growth factor. *Proc. Natl. Acad. Sci.* 73, 2424–2428.
- Groh, C., Lu, Z., Meinertzhagen, I.A., Rössler, W., 2012. Age-related plasticity in the synaptic ultrastructure of neurons in the mushroom body calyx of the adult honeybee *Apis mellifera*. *J. Comp. Neurol.* 520, 3509–3527.
- Groh, C., Rössler, W., 2008. Caste-specific postembryonic development of primary and secondary olfactory centers in the female honeybee brain. *Arthropod Struct. Dev.* 37, 459–468.
- Hansson, B.S., Anton, S., 2000. Function and morphology of the antennal lobe: new developments. *Annu. Rev. Entomol.* 45, 203–231.
- Hanström, B., 1928. Vergleichende Anatomie des Nervensystems der wirbellosen Tiere.
- Haubensak, W., Attardo, A., Denk, W., Huttner, W.B., 2004. Neurons arise in the basal neuroepithelium of the early mammalian telencephalon: a major site of neurogenesis. *Proc. Natl. Acad. Sci. U.S.A.* 101, 3196–3201.
- Hein, K., Mittler, G., Gizelsky, W., Kühl, M., Ferrante, F., Liefke, R., Berger, I.M., Just, S., Sträng, J.E., Kestler, H.A., 2015. Site-specific methylation of Notch1 controls the amplitude and duration of the Notch1 response. *Sci. Signal.* 8, ra30-ra30.
- Heisenberg, M., 1998. What do the mushroom bodies do for the insect brain? An introduction. *Learn. Memory* 5, 1–10.
- Held, M., Berz, A., Hensgen, R., Muenz, T.S., Scholl, C., Rössler, W., Homberg, U., Pfeiffer, K., 2016. Microglomerular synaptic complexes in the sky-compass network of the honeybee connect parallel pathways from the anterior optic tubercle to the central complex. *Front. Behav. Neurosci.* 10, 186.
- Hirota, K., Shigekawa, C., Araoi, S., Sha, L., Inagawa, T., Kanou, A., Kako, K., Daitoku, H., Fukamizu, A., 2017. Simultaneous ablation of prmt-1 and prmt-5 abolishes asymmetric and symmetric arginine dimethylations in *Caenorhabditis elegans*. *J. Biochem.* 161, 521–527.
- Homem, C.C., Knoblich, J.A., 2012. *Drosophila* neuroblasts: a model for stem cell biology. *Development* 139, 4297–4310.
- Homem, C.C., Steinmann, V., Burkard, T.R., Jais, A., Esterbauer, H., Knoblich, J.A., 2014. Ecdysone and mediator change energy metabolism to terminate proliferation in *Drosophila* neural stem cells. *Cell* 158, 874–888.
- Huang, J., Vogel, G., Yu, Z., Almazan, G., Richard, S., 2011. Type II arginine methyltransferase PRMT5 regulates gene expression of inhibitors of differentiation/DNA binding Id2 and Id4 during glial cell differentiation. *J. Biol. Chem.* 286, 44424–44432.
- Iacopetti, P., Michelini, M., Stuckmann, I., Oback, B., Aaku-Saraste, E., Huttner, W.B., 1999. Expression of the antiproliferative gene TIS21 at the onset of neurogenesis identifies single neuroepithelial cells that switch from proliferative to neuron-generating division. *Proc. Natl. Acad. Sci.* 96, 4639–4644.
- Jay, S.C., 1962. Colour changes in honeybee pupae. *Bee World* 43, 119–122.
- Kenyon, F., 1896. The brain of the bee. A preliminary contribution to the morphology of the nervous system of the Arthropoda. *J. Comp. Neurol.* 6, 133–210.
- Kimura, S., Sawatsubashi, S., Ito, S., Kouzmenko, A., Suzuki, E., Zhao, Y., Yamagata, K., Tanabe, M., Ueda, T., Fujiyama, S., 2008. *Drosophila* arginine methyltransferase 1 (DART1) is an ecdysone receptor co-repressor. *Biochem. Biophys. Res. Commun.* 371, 889–893.
- Kohno, H., Suenami, S., Takeuchi, H., Sasaki, T., Kubo, T., 2016. Production of Knockout Mutants by CRISPR/Cas9 in the European Honeybee, *Apis mellifera* L. *Zool. Sci.* 33, 505–512.
- Krause, C.D., Yang, Z.-H., Kim, Y.-S., Lee, J.-H., Cook, J.R., Pestka, S., 2007. Protein arginine methyltransferases: evolution and assessment of their pharmacological and therapeutic potential. *Pharmacol. Ther.* 113, 50–87.
- Kunz, T., Kraft, K.F., Technau, G.M., Urbach, R., 2012. Origin of *Drosophila* mushroom body neuroblasts and generation of divergent embryonic lineages. *Development dev.* 077883.
- Kurshan, P.T., Hamilton, I.S., Mustard, J.A., Mercer, A.R., 2003. Developmental changes in expression patterns of two dopamine receptor genes in mushroom bodies of the honeybee, *Apis mellifera*. *J. Comp. Neurol.* 466, 91–103.
- Li, L., Su, S., Perry, C.J., Elphick, M.R., Chittka, L., Søvik, E., 2018. Large-scale transcriptome changes in the process of long-term visual memory formation in the bumblebee, *Bombus terrestris*. *Sci. Rep.* 8, 534.
- Lin, W.-J., Gary, J.D., Yang, M.C., Clarke, S., Herschman, H.R., 1996. The mammalian immediate-early TIS21 protein and the leukemia-associated BTG1 protein interact with a protein-arginine N-methyltransferase. *J. Biol. Chem.* 271, 15034–15044.
- Malun, D., 1998. Early development of mushroom bodies in the brain of the honeybee *Apis mellifera* as revealed by BrdU incorporation and ablation experiments. *Learn. Memory* 5, 90–101.
- Malun, D., Moseleit, A.D., Grünwald, B., 2003. 20-hydroxyecdysone inhibits the mitotic activity of neuronal precursors in the developing mushroom bodies of the honeybee, *Apis mellifera*. *J. Neurobiol.* 57, 1–14.
- Miyata, S., Mori, Y., Tohyama, M., 2008. PRMT1 and Btg2 regulates neurite outgrowth of Neuro2a cells. *Neurosci. Lett.* 445, 162–165.
- Neuser, K., Triphan, T., Mronz, M., Poeck, B., Strauss, R., 2008. Analysis of a spatial orientation memory in *Drosophila*. *Nature* 453, 1244.
- Pan, Y., Zhou, Y., Guo, C., Gong, H., Gong, Z., Liu, L., 2009. Differential roles of the fan-shaped body and the ellipsoid body in *Drosophila* visual pattern memory. *Learn. Memory* 16, 289–295.
- Pawlak, M.R., Scherer, C.A., Chen, J., Roshon, M.J., Ruley, H.E., 2000. Arginine N-methyltransferase 1 is required for early postimplantation mouse development, but cells deficient in the enzyme are viable. *Mol. Cell. Biol.* 20, 4859–4869.

- Plath, J.A., Entler, B.V., Kirkerud, N.H., Schlegel, U., Galizia, C.G., Barron, A.B., 2017. Different roles for honey bee mushroom bodies and central complex in visual learning of colored lights in an aversive conditioning assay. *Front. Behav. Neurosci.* 11, 98.
- Pouvreau, A., 1989. Contribution à l'étude du polyéthisme chez les bourdons, *Bombus Latr.* (Hymenoptera, Apidae). *Apidologie* 20, 229–244.
- Prýs-Jones, Oliver E., Corbet, S.A., 2003. *Bumblebees*. The Richmond Publishing Co. Ltd.
- R Core Team, 2017. *R: A Language and Environment for Statistical Computing*. R Foundation for Statistical Computing, Vienna, Austria.
- Riveros, A.J., Gronenberg, W., 2010. Brain allometry and neural plasticity in the bumblebee *Bombus occidentalis*. *Brain Behav. Evol.* 75, 138–148.
- Roat, T.C., da Cruz Landim, C., 2010. Differences in mushroom bodies morphogenesis in workers, queens and drones of *Apis mellifera*: neuroblasts proliferation and death. *Micron* 41, 382–389.
- Rybak, J., Menzel, R., 2010. Mushroom body of the honeybee. In: *Handbook of Brain Microcircuits*, pp. 433–438.
- Schindelin, J., Arganda-Carreras, I., Frise, E., Kaynig, V., Longair, M., Pietzsch, T., Preibisch, S., Rueden, C., Saalfeld, S., Schmid, B., 2012. Fiji: an open-source platform for biological-image analysis. *Nat. Methods* 9, 676–682.
- Selvi, B.R., Swaminathan, A., Maheshwari, U., Nagabhushana, A., Mishra, R.K., Kundu, T.K., 2015. CARM1 regulates astroglial lineage through transcriptional regulation of Nanog and posttranscriptional regulation by miR92a. *Mol. Biol. Cell* 26, 316–326.
- Siegrist, S.E., Haque, N.S., Chen, C.-H., Hay, B.A., Hariharan, I.K., 2010. Inactivation of both Foxo and reaper promotes long-term adult neurogenesis in *Drosophila*. *Curr. Biol.* 20, 643–648.
- Simandi, Z., Czipa, E., Horvath, A., Koszeghy, A., Bordas, C., Póliska, S., Juhász, I., Imre, L., Szabó, G., Dezsó, B., 2015. PRMT1 and PRMT8 regulate retinoic acid-dependent neuronal differentiation with implications to neuropathology. *Stem cells* 33, 726–741.
- Stolle, E., Wilfert, L., Schmid-Hempel, R., Schmid-Hempel, P., Kube, M., Reinhardt, R., Moritz, R.F., 2011. A second generation genetic map of the bumblebee *Bombus terrestris* (Linnaeus, 1758) reveals slow genome and chromosome evolution in the Apidae. *BMC Genomics* 12, 48.
- Takahashi, Y., Daitoku, H., Hirota, K., Tamiya, H., Yokoyama, A., Kako, K., Nagashima, Y., Nakamura, A., Shimada, T., Watanabe, S., 2011. Asymmetric arginine dimethylation determines life span in *C. elegans* by regulating forkhead transcription factor DAF-16. *Cell Metab.* 13, 505–516.
- Tee, W.-W., Pardo, M., Theunissen, T.W., Yu, L., Choudhary, J.S., Hajkova, P., Surani, M.A., 2010. Prmt5 is essential for early mouse development and acts in the cytoplasm to maintain ES cell pluripotency. *Genes Dev.* 24, 2772–2777.
- Wang, Y.C., Li, C., 2012. Evolutionarily conserved protein arginine methyltransferases in non-mammalian animal systems. *FEBS J.* 279, 932–945.
- Yadav, N., Lee, J., Kim, J., Shen, J., Hu, M.C.-T., Aldaz, C.M., Bedford, M.T., 2003. Specific protein methylation defects and gene expression perturbations in coactivator-associated arginine methyltransferase 1-deficient mice. *Proc. Natl. Acad. Sci.* 100, 6464–6468.
- Yan, H., Opachaloemphan, C., Mancini, G., Yang, H., Gallitto, M., Mlejnek, J., Leibholz, A., Haight, K., Ghaninia, M., Huo, L., 2017. An engineered orco mutation produces aberrant social behavior and defective neural development in ants. *Cell* 170, 736–747 e739.